Influence of continental air mass transport on atmospheric CO_2 in the western North Pacific

Akira Wada,[1] Yousuke Sawa,[2] Hidekazu Matsueda,[2] Shoichi Taguchi,[3] Shohei Murayama,[3] Saki Okubo,[4] and Yukitomo Tsutsumi[5]

Received 24 May 2006; revised 6 October 2006; accepted 29 October 2006; published 12 April 2007.

[1] Since 1993, atmospheric carbon dioxide (CO_2) has been continuously observed by the Japan Meteorological Agency at Minamitorishima station (24°18′N, 153°58′E), located about 2000 km off the Asian continent in the western North Pacific. The long-term record shows high-frequency measurements with interesting episodic events with extremely low CO_2 mixing ratios 5–10 ppm below the background seasonal cycle. These extremely low CO_2 (ELC) events occur several times each year, primarily in July, August, and September, although the number of events varies from year to year. The origins of air masses associated with the ELC events were defined by backward trajectory analyses as well as chemical characterizations using simultaneous observations of other trace gases (CO, CH_4, and O_3). The results indicate that the air masses with extremely low CO_2 were influenced by active biospheric uptake in summer over different continental sink regions in Siberia, northern Asia, and Southeast Asia due to rapid long-range transport driven by strong northerly or southerly winds. The spatial scale of the widespread low-CO_2 distribution for the ELC events in 2001 was captured by a simulation experiment using a three-dimensional chemical transport model. It clearly revealed that the Intertropical Convergence Zone around 20°N in the western North Pacific during summer blocked further southward intrusion of ELC events through the lower troposphere.

Citation: Wada, A., Y. Sawa, H. Matsueda, S. Taguchi, S. Murayama, S. Okubo, and Y. Tsutsumi (2007), Influence of continental air mass transport on atmospheric CO_2 in the western North Pacific, *J. Geophys. Res.*, *112*, D07311, doi:10.1029/2006JD007552.

1. Introduction

[2] Global levels of atmospheric carbon dioxide (CO_2) concentration have increased more than 30% since the preindustrial era because of fossil fuel combustion and deforestation by human activities. This increase will likely cause changes in global climate because CO_2 is estimated to have the largest contribution to anthropogenic radiative forcing. The CO_2 annual growth rate during the 1990s varied interannually from 0.9 to 2.8 ppm yr^{-1}, which is equivalent to 1.9 to 6.0 PgC yr^{-1} [*Intergovernmental Panel on Climate Change*, 2001], but many uncertainties remain regarding the prediction of annual changes in the CO_2 uptake by the land biosphere and ocean. An increase in atmospheric observations, in conjunction with improved global carbon cycle models, is needed to better constrain the CO_2 sources and sinks.

[3] Temporal and spatial variations of atmospheric CO_2 have been observed by using ground-based monitoring stations [e.g., *Tanaka et al.*, 1987a; *Nakazawa et al.*, 1991a; *Conway et al.*, 1994], aircraft [e.g., *Tanaka et al.*, 1989; *Nakazawa et al.*, 1991b; *Matsueda et al.*, 2002], and ships [e.g., *Tanaka et al.*, 1987b]. Most of the data from these observations were collected weekly or biweekly using flasks. However, flask sampling observations alone are inadequate for a full understanding of the large CO_2 variations associated with atmospheric transport processes on a synoptic or shorter timescale. *Murayama et al.* [2003] pointed out that sampling at an interval longer than such a synoptic timescale could lead to biased estimates of the interannual trend and seasonal cycle. It has also been reported that changes in the atmospheric circulation could contribute significantly to the observed year-to-year change in atmospheric CO_2 [*Higuchi et al.*, 2002; *Murayama et al.*, 2004]. These studies indicate that high-frequency measurements from in situ continuous measurement systems are needed to elucidate the carbon cycle more precisely.

[4] CO_2 data are also essential for inversion modeling studies to estimate regional CO_2 sources and sinks. Previous inversion models used monthly mean data calculated from smoothed curve-fitting techniques to remove the influence

[1]Meteorological College, Kashiwa, Japan.
[2]Geochemical Research Department, Meteorological Research Institute, Tsukuba, Japan.
[3]National Institute of Advanced Industrial Science and Technology, Tsukuba, Japan.
[4]Nagano Local Meteorological Observatory, Japan Meteorological Agency, Nagano, Japan.
[5]Global Environment and Marine Department, Japan Meteorological Agency, Tokyo, Japan.

0148-0227/07/2006JD007552

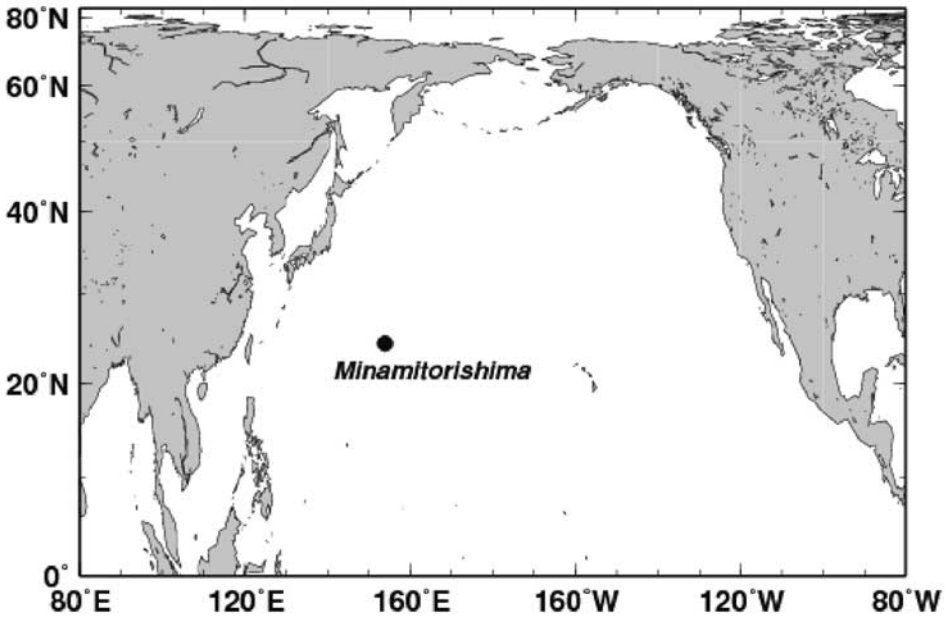

Figure 1. Map showing the geographical location of Minamitorishima station (24°18′N, 153°58′E, 9 m above sea level).

of nonbaseline variations from outlying measurements [e.g., *Bousquet et al.*, 2000]. However, *Law et al.* [2002] reported that the uncertainties of CO_2 flux estimations were reduced by using nonbaseline data for an inversion model. It has been strongly suggested that the use of outlying data on shorter timescales from high-frequency observations could potentially result in a more accurate estimate of the CO_2 sources and sinks [*Gurney et al.*, 2002].

[5] In the western Pacific, large temporal and spatial variations of CO_2 and other trace gases are often observed with episodic events due to the continental outflow [e.g., *Pochanart et al.*, 1999; *Jaffe et al.*, 1997; *Bey et al.*, 2001; *Liu et al.*, 2003; *Sawa et al.*, 2004], from Asia which experiences both strong anthropogenic emissions and a land-biospheric source and sink region. In addition, midlatitude synoptic weather changes can cause larger short-term variation in the atmospheric trace gases in the western North Pacific. The influence of an Asian outflow by long-range transport to the central Pacific has been clearly revealed in previous studies [e.g., *Harris et al.*, 1992; *Murayama et al.*, 2003]. However, a detailed study of the air transport associated with shorter time variations of atmospheric CO_2 in the western North Pacific has not been done.

[6] Since 1994, the Japan Meteorological Agency (JMA) has been monitoring atmospheric CO_2 at Minamitorishima station on a remote coral island in the western North Pacific using a continuous measurement instrument [*Watanabe et al.*, 2000]. This long-term record with high-frequency measurements is useful for investigating the shorter time variation of CO_2 relating to the long-range transport of the Asian continental outflow. In this study, we focus on extremely low CO_2 events observed at Minamitorishima station and examine their origins and transport in detail. The seasonal and interannual occurrences of the low-CO_2 events are first analyzed using data from 1994–2004. Second, the origins are examined by backward trajectory analysis as well as chemical characterization of other trace gases observed simultaneously at this station. Third, the transport pathways and mechanism are analyzed using weather charts as well as a three-dimensional chemical transport model.

2. Methods

2.1. Monitoring Site

[7] The station of Minamitorishima (24°18′N, 153°58′E, 9 m above sea level) is situated on a remote coral island in the western North Pacific, about 2000 km southeast of Tokyo (Figure 1). This station has been operated by the Japan Meteorological Agency (JMA) for long-term observations of atmospheric trace gases under the Global Atmosphere Watch program of the World Meteorological Organization (WMO/GAW). The island has an area of 1.4 km^2 and is covered with sparse evergreen shrub and grass. Approximately 50 people from the JMA are dispatched to the site each year, in addition to people sent by the Japanese Marine Self-Defense Force and Coast Guard. Because the island is in the subtropical region and located on the southern edge of the Pacific high, maritime air from easterly winds prevails throughout the year. Continental air masses from East Asia are sometimes transported by the synoptic-scale weather perturbations, but the influences of local sources and sinks within this small island are negligible for trace gas observations.

2.2. Sampling and Measuring Methods

[8] At the Minamitorishima station, carbon dioxide (CO_2), carbon monoxide (CO), methane (CH_4), and ozone (O_3) have been measured by the Atmospheric Environmental Division of JMA since March 1993. Since details of

continuous measurement systems have been previously reported by *Japan Meteorological Agency* [1994] and *Watanabe et al.* [2000], only brief descriptions of the analytical methods are given here.

[9] Sample air is collected from the top of a 10 m observational tower. After drying the sample air, the CO_2 concentration is measured using a nondispersive infrared analyzer (NDIR: VIA510R, Horiba, Ltd., Japan) with the analytical precision of about 0.02 ppm. All CO_2 measurements used here were recalculated for consistency with the WMO CO_2 mole fraction scale from the National Oceanic and Atmospheric Administration/Global Monitoring Division (NOAA/GMD, formerly NOAA/CMDL) [*Matsueda et al.*, 2004a]. CO and CH_4 are measured continuously using an NDIR (GA-360S, Horiba, Ltd., Japan) with the overall analytical precision of about ± 5 ppb. The concentration of CH_4 in the sample air is reported on the JMA primary standard scale [*Matsueda et al.*, 2004b], which is similar to the WMO CH_4 mole fraction scale from the NOAA/GMD [*Dlugokencky et al.*, 2005]. The concentration of CO in the sample air is determined by standard gases assigned by the Chemicals Evaluation and Research Institute of Japan.

[10] Sample air for the O_3 measurement is provided using a different inlet installed on the top of the observatory building. O_3 is measured using an ozone analyzer (EG2001F, Ebara Jitsugyo Co., Ltd., Japan) with the overall precision of less than 1%.

2.3. Observational Data

[11] The output data from the NDIR analyzers for the CO_2, CO, and CH_4 measurements are collected by data loggers every second and then averaged for 30 s to calculate the concentrations on the basis of regular measurements of the working standards. The O_3 concentration is averaged for 15 s and directly obtained from the analyzer. These averaged data sets along with their standard deviations are used to perform careful quality assurance tests before generating hourly data sets at JMA. The data are posted on the WMO World Data Center for Greenhouse Gases (WMO/WDCGG, http://gaw.kishou.go.jp/wdcgg.html) operated by the JMA in Tokyo. In this study, hourly data sets for CO_2, CO, CH_4, and O_3 observed at the Minamitorishima station for 12 years between March 1993 and December 2004 are used.

2.4. Trajectory Analysis

[12] We applied a 10-day isentropic backward trajectory analysis to examine the transport pathways associated with observed trace gas variations. Although the assumption of the adiabatic processes does not necessarily account for the movement of air parcels which are accompanied by precipitation or strong wind shear, this assumption is acceptable on a synoptic scale of air motion in the free troposphere [*Harris and Kahl*, 1990]. The trajectory model used here was developed at the Meteorological Research Institute, as reported in detail by *Sawa* [2005]. In this model, the global analysis data (GANAL) prepared by JMA was used as meteorological data for the trajectory calculation. The spatial resolution of the GANAL data was 1.25° × 1.25° after March 1996 and 1.875° × 1.875° prior to March 1996. The number of vertical layers is 18, with time intervals of 6 hours after March 1996 and 12 hours prior to March 1996.

[13] Although the Minamitorishima station is located near the zero level, the trajectories were calculated at an altitude level of 1500 m in order to obtain a more representative transport pathway in the boundary layer. To assess the precision of trajectory analysis, we compared five trajectories at a center and four end points located in a 0.5° × 0.5° box with the actual observation site. When the pathways of the five trajectories were quite distinct, the trajectories were not used for the interpretation of the air mass origins in the present study.

2.5. The 3-D Transport Model

[14] To quantitatively understand the spatial scale for the CO_2 variations observed at Minamitorishima, a 3-D chemical transport model was used in this study. The model of the NIRE-CTM-96 was developed at the National Institute of Advanced Industrial Sciences and Technology (AIST, the former National Institute for Research and Environment) in Japan [*Taguchi*, 1996; *Taguchi et al.*, 2002a]. This model has 1.125° horizontal resolution with 60 vertical levels, and its advection is calculated by using a semi-Lagrangian scheme. The model was compared with other models used in international model intercomparison studies of the TransCom experimental series to characterize model behavior [*Gurney et al.*, 2004]. In addition, model validations were conducted by comparisons with observed data of CO_2, CO, and radon [*Taguchi et al.*, 2002a, 2002b, 2003]. In this study, the model calculation was driven by the meteorological data from NCEP/NCAR with the biospheric exchange data of CO_2 from the Carnegie Ames Stanford Approach (CASA) model [*Randerson et al.*, 1997]. The other experiment was also performed using the same model with total CO_2 fluxes including biospheric exchange, fossil fuel emissions [*Andres et al.*, 1996], and oceanic exchange of CO_2 [*Takahashi et al.*, 2002].

3. Results and Discussion

3.1. CO_2 Variations

[15] Figure 2 shows the hourly mean CO_2 observed at the Minamitorishima station from March 1993 to December 2004. The CO_2 record clearly shows a long-term increasing trend, a distinct seasonal cycle, and high-frequency short-term variations. The CO_2 data record contains a minimal diurnal signal with a mean amplitude of 0.6 ppm found throughout the year. The data have also been examined for local sources and sinks for the CO_2. It is clear that neither the diurnal signal or local signal can account for the episodic behavior.

[16] The annual mean level of CO_2 indicates a continuous increase from 360 ppm in 1994 to 378 ppm in 2004. The averaged growth rate during the 11 years period (1994–2004) is about 1.8 ppm yr^{-1}, with large interannual variation of the CO_2 growth rate from about 1 ppm yr^{-1} in 1996 to 3 ppm yr^{-1} around 1997–1998 and 2002–2003. A similar increasing CO_2 trend and interannual variability has been observed by the wide-coverage observations from the JAL airliner [*Matsueda et al.*, 2002] and from the ground-based flask sampling network of NOAA/GMD [*Conway et al.*, 1994].

[17] The averaged seasonal cycle shows a minimum in mid-September and a maximum in mid-May with a mean

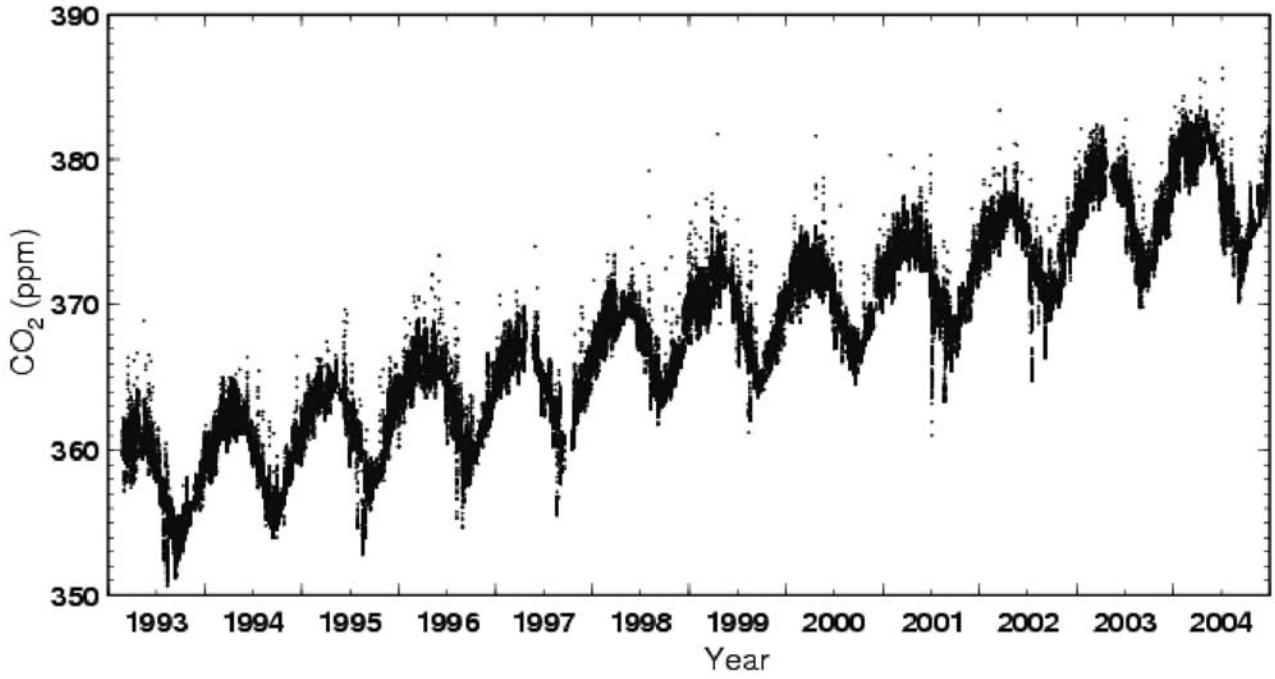

Figure 2. Hourly CO_2 data observed at Minamitorishima from March 1993 to December 2004. During this period, no measurements are available for May–June in 1995, April–May in 1997, September–October in 1997, and April–May in 2003 because of maintenance or problems with the CO_2 measurement system.

peak-to-peak amplitude of about 7 ppm (Figure 2). The average seasonality observed at Minamitorishima is similar to that observed at Cape Kumukahi in Hawaii, located in the same subtropical North Pacific [*Conway et al.*, 1994], but larger year-to-year variation of the seasonal cycle amplitude was found at the Minamitorishima station, with the most significant feature being a large change of the level of the seasonal minimum due to sharp decreased CO_2 peaks in the summer and early fall (Figure 2). Relatively larger reductions of the CO_2 seasonal minimum were found in 1993, 1995, 1996, 1997, 2001, and 2002, while the seasonal cycles in 1994, 1998, and 2000 showed no significant reduction of the CO_2 minimum relative to Cape Kumukahi. This yearly change is caused by short-term variations on timescales between several days and weeks due to synoptic-scale intrusions of low-CO_2 air masses to the station in summer. Another change of the seasonal cycle pattern was found in 1996 and 2000, when a submaximum in mid-March was relatively more enhanced than the usual maximum in mid-May. This was caused by the frequent elevations due to synoptic-scale transport of air masses with higher CO_2 in early spring. The seasonal cycle pattern at the Minamitorishima station varies from year to year because of short-term variations associated with regional air circulation in the western North Pacific.

3.2. Extremely Low CO_2 Event

[18] Figure 3a shows details of the short-term variation of CO_2 using data from 2001. This 1-year data set shows a well-defined seasonal cycle as well as numerous short-term variations consisting of both negative and positive peaks on timescales less than one week. Typical peak-to-peak amplitudes are less than 2 ppm (Figure 3a). However there are two larger negative peaks with much lower CO_2 of approximately 8 ppm in early July and 5 ppm in late August.

[19] Since this study focuses on extremely low CO_2 events, it is necessary to separate these from the typical short-term variation. To do this, we applied a median filter for 40 days followed by a running mean for 40 days to the hourly data set to calculate a fitting curve for the seasonal cycle. The median filter was used to minimize the influence of larger outliers before the running mean. The fitting curve determined from this procedure accurately represented the smoothed seasonal variation, including the long-term trend component in 2001 (Figure 3a). The differences between the hourly data and the smoothed seasonal curve were calculated as residual CO_2 (ΔCO_2), which is plotted in Figure 3b to investigate an occurrence pattern of the low CO_2 peaks.

[20] Similar events with large drops in CO_2 (as in 2001) are also found in other years. In order to distinguish an event with extremely low CO_2 (ELC) from many of the smaller negative peaks, we chose to use the following criteria of ΔCO_2. (1) ΔCO_2 that decreased below -3.1 ppm, which was 3σ of all ΔCO_2 values, was extracted during the entire period. (2) The extracted ΔCO_2 was regarded as a peak for an ELC event if it lasted for more than two hours. (3) When a peak-to-peak interval was more than four hours long, it was identified as a different peak. According to these criteria, 40 ELC events were identified from the 11 year measurement record (1994–2004).

[21] As shown in Figure 4 the ELC events occurred primarily in the summer season with 43% of the ELCs in July, 35% in August, and 18% in September. ELC events in

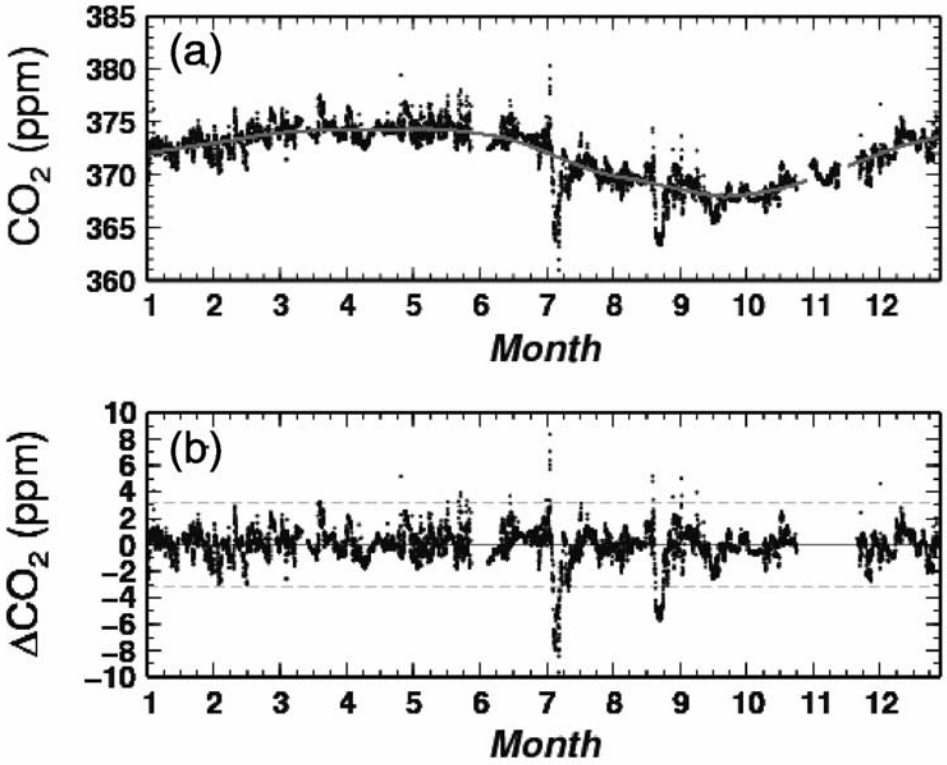

Figure 3. (a) Observed hourly CO_2 data (dots) and smoothed seasonal curve (solid line) at Minamitorishima in 2001. A detailed procedure describing the seasonal curve analysis is included in the text. (b) Residual CO_2 (ΔCO_2) data (dots) from the differences between the hourly data and the seasonal curve and a range of ΔCO_2 variability (dotted lines) within ± 3.1 ppm, using data in Figure 3a.

other months were rare (<3%). The peaks in winter with averaged ΔCO_2 of −3.5 ppm were smaller than those observed in summer. The yearly frequency of the ELC events contains a large interannual variation with the number of events being 5–7 in 1995, 1996, 2002, and 2004, with fewer than 3 events in each of 1994, 1997, 1998, and 2003. The magnitude of ΔCO_2 minimum for the ELC events also varied year by year with the ΔCO_2 minimum ranging from 4 to 10 ppm, and not related to the yearly variation of the number of the ELC events. These results suggest that conditions favorable for the transport of low-CO_2 air masses to Minamitorishima occur in the summer over the western North Pacific with significant year-to-year variability.

3.3. Origin of Air Masses With Low CO_2

[22] We examined the 10-day isentropic backward trajectories for all ELC events in order to deduce the most likely origins for the air masses with extremely low CO_2. Since the trajectories were calculated at an interval of 6 hours, several trajectories were obtained for each event. Figure 5 shows all of the trajectories classified into 5 trajectory origin sectors, i.e., north (N), west (W), south (S), east (E), and complex (C). Trajectories were assigned when they passed over the

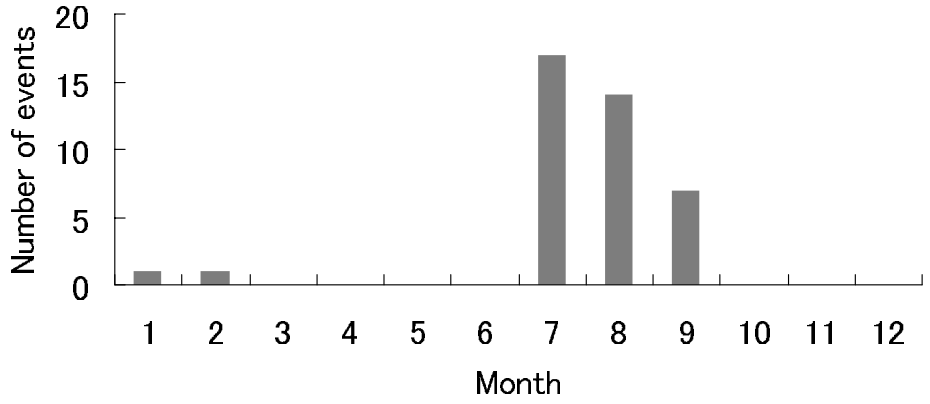

Figure 4. Seasonal variation of the number of the extremely low CO_2 (ELC) events during 1994–2004.

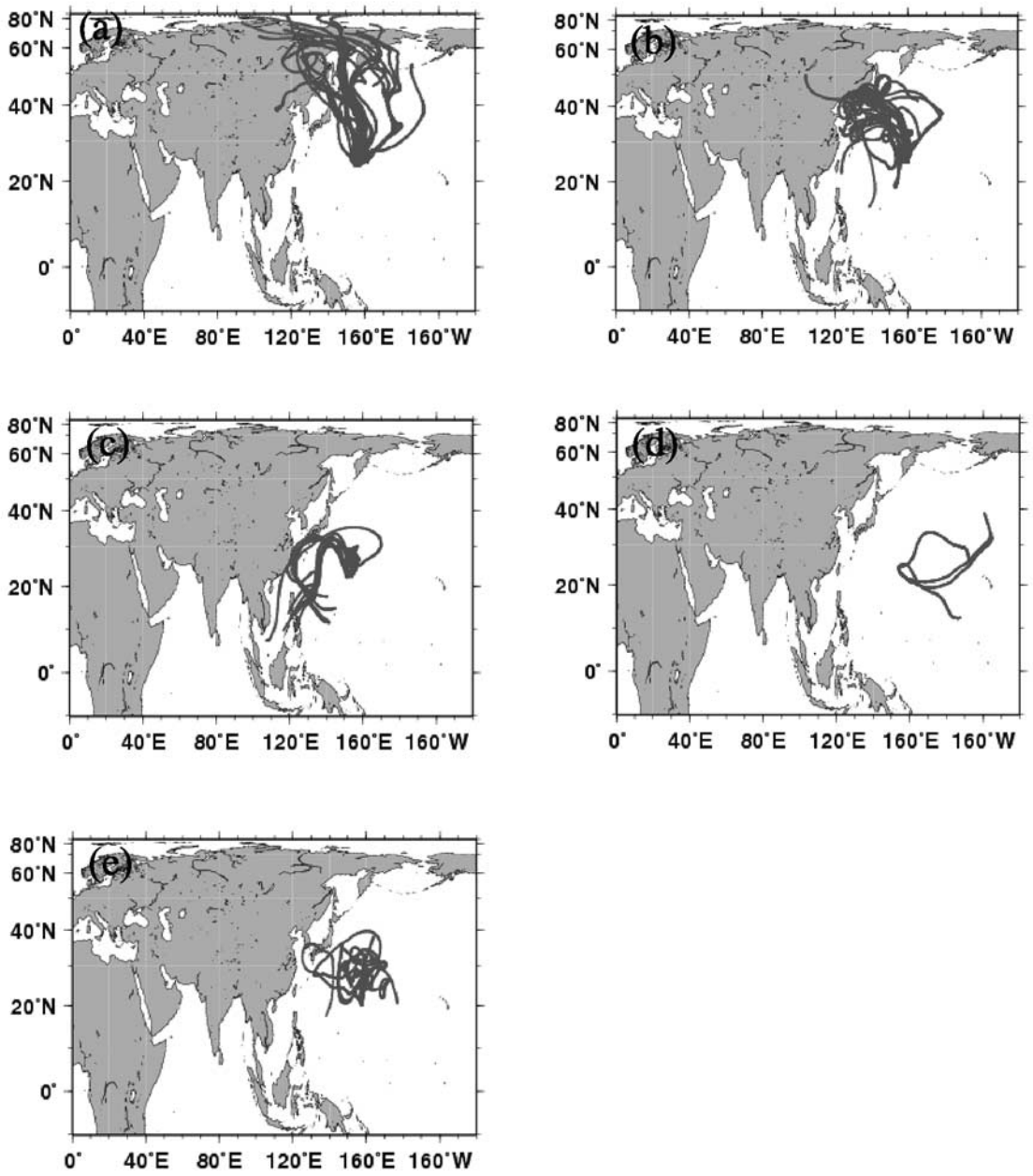

Figure 5. The 10-day isentropic backward trajectories for the ELC events classified into five sectors: (a) north (N), (b) west (W), (c) south (S), (d) east (E), and (e) complex (C). Detailed classification procedures for the trajectory sectors are described in the text.

area of each sector. The range of the area was defined as 50°N–80°N and 100°E–160°W for the N sector, 20°N–50°N and 100°E–130°E for the W sector, 20°N–0° and 100°E–130°E for the S sector, and 50°N–0° and 180°–160°W for the E sector. Others were classified as the C sector.

[23] The trajectories for the N sector clearly show the low-CO_2 air masses originated from the higher latitudes around Siberia as well as from the Bering Sea. It is most likely that extremely low CO_2 was produced by active uptake from boreal forests in Siberia in summer and then flowed out into the oceanic region around the Bering Sea. In the case of the trajectories for the W sector, the air masses were transported from the directions of northern China and Japan, where the CO_2 concentration likely decreased as a result of uptake by the temperate mixed forests. The trajectories for the S sector showed that the air masses were transported from the directions of the tropical forests in Southeast Asia and/or southern China in East Asia. Thus it is likely that active uptake by the land biosphere in summer generated continental air masses for the ELC events in the trajectories for the N, W, and S sectors. However, no strong sink regions for the E and C sectors could be identified by the 10-day trajectories because maritime air masses dominated in both sectors. *Murayama et al.* [2003] reported that large CO_2 variations were observed episodically by ship-

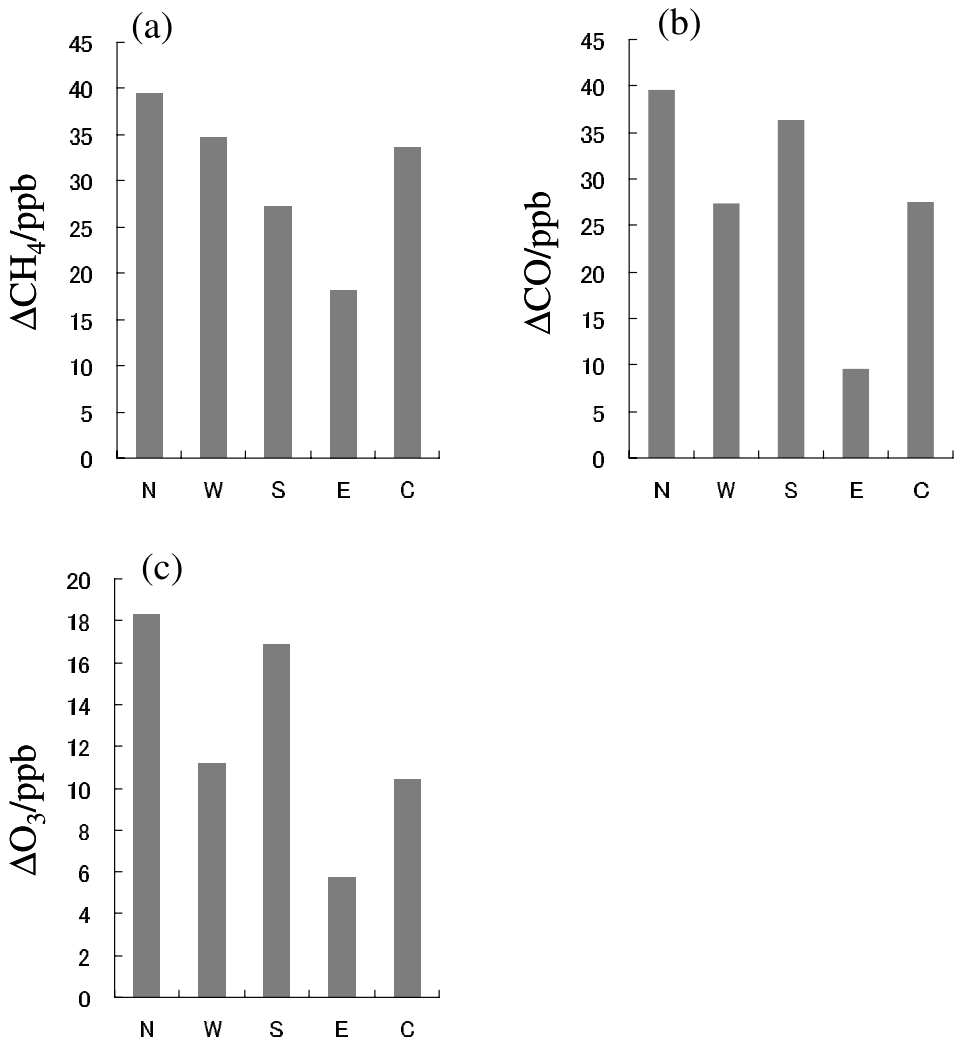

Figure 6. Enhanced mixing ratios of (a) ΔCH_4, (b) ΔCO, and (c) ΔO_3 for five trajectory types of N, W, S, E, and C for the ELC events. Detailed calculation procedures for the trace gas enhancements are described in the text.

board observations around a synoptic-scale front on the central Pacific, but no front system was found on the weather charts around Minamitorishima before the observed ELC events in the present study.

[24] The yearly frequency of the 5 different transport pathways largely depended on the years from 1994 to 2004. In 1995, 1997, 2002, and 2003, continental air masses for the N or W sectors accounted for 60–100% of the total ELC events. The pathways for the S sector occupied 50% in 1999. In 1995, 1996, 1999, and 2001, various transport pathways are included. This result suggested that sink regions for the low CO_2 in the ELC events were changed by a regional weather system in the western North Pacific year by year. When we examined a monthly frequency of the 5 transport pathways, the predominant pathways for the ELC events varied much from month to month. About one half of the trajectories in July showed transport from the W sector, while the transport from the N sector was predominant in August. In September, both trajectories for the W and N sectors decreased, with the primary transport pathway originating from the C sector. Thus differences indicated that the air mass origin for the ELC event varied from month to month because of a seasonal change of the weather system in the western North Pacific.

3.4. Enhancement of Other Trace Gases

[25] We find that CH_4, CO, and O_3 are simultaneously enhanced when ELC events are observed at the Minamitorishima station. Enhanced concentrations are calculated as ΔCO, ΔCH_4, and ΔO_3 using the same procedure applied to CO_2. Figure 6 shows the mean ΔCH_4, ΔCO, and ΔO_3 for the five transport pathways from the N, W, S, E, and C sectors in the ELC events from 1994 to 2004. The mean values were obtained from averaging all enhanced concentrations corresponding to the ΔCO_2 below −3.1 ppm, as the criteria of the ELC events. The results clearly show that the ΔCH_4, ΔCO, and ΔO_3 were different among the air mass origins classified by the trajectory analyses because the geographical distribution of sources and sinks largely influences these trace gases.

[26] For ΔCH_4, relatively larger enhancements of 30 to 40 ppb were found in air masses from the N and W sectors. This result suggests that the enhanced CH_4 in both the N and W sectors was influenced by increased CH_4 emissions

from wetlands in Siberia in summer [*Fung et al.*, 1991; *Dlugokencky et al.*, 1994]. Another cause is the transport of the air masses from northern high latitudes as a source of CH_4 due to the north-to-south gradient for background CH_4 which has a latitudinal difference of around 40 ppb between 50°N and 20°N in summer [*Dlugokencky et al.*, 1994]. In contrast, the ΔCH_4 for the pathway from the S sector shows a relatively smaller enhancement, suggesting the different air mass origin.

[27] For ΔCO, a smaller enhancement of less than 10 ppb was found in the transport in the E sector, but other pathways showed enriched-CO air masses with ΔCO of 35 to 40 ppb for the N and S sectors, and about 26 ppb for the W and C sectors. The CO enhancements are caused by polluted air masses from East Asia and Southeast Asia [*Bey et al.*, 2001; *Jaffe et al.*, 1997; *Liu et al.*, 2003] and/or the substantial north-to-south gradient of around 30 ppb between 50°N and 20°N in summer [*Novelli et al.*, 2003]. This indicates that most of the air masses with higher ΔCO were transported from the continent or northern higher latitudes.

[28] For ΔO_3, relatively higher values of more than 15 ppb were found in the air masses from the N and S sectors. These O_3 enhancements are associated with higher levels of ΔCO, suggesting the photochemical production of O_3 during transport to Minamitorishima. In addition, the larger ΔO_3 was partly influenced by the steep north-to-south gradient in the western North Pacific in summer [*Tanimoto et al.*, 2005].

[29] The origins of the air masses from both the C and E sectors are not well defined by the 10-day trajectory analyses, but the chemical compositions of the ΔCH_4, ΔCO, and ΔO_3 indicated a large difference in the two cases. The larger enhancements of ΔCH_4 and ΔCO in the case of C were similar to those in the cases of the N and W, strongly suggesting that the air masses originated from the continent or higher latitudes. On the other hand, the lower ΔCH_4, ΔCO, and ΔO_3 in the case of the E sector were associated with the smaller ΔCO_2 decreases for the ELC events. It is likely that dilution by maritime air would diminish the continental signal.

3.5. Transport Mechanism of Low CO_2

[30] In order to clarify the detailed transport mechanism for the ELC events, we investigated weather charts over the western North Pacific and compared them with the transport pathways calculated from the backward trajectories. As a result of this approach, a specific weather system could be identified for each transport pathway in summer. The weather charts were created by the JMA.

[31] As an example of transport from N sector, Figures 7a and 7b show the weather charts at 0000 UTC on 17 and 19 August 2001 before the ELC event observed on 21 August at Minamitorishima. The trajectory analysis for this event indicated that air masses were transported southward from Siberia to Minamitorishima. In the weather chart on 17 August, 4 days before the event, it clearly shows that the air parcel around 45°N was located between the high-pressure system over the Amur River and the low-pressure system over the Kamchatka Peninsula. This air parcel rapidly moved southward to about 31°N in about 2 days through the pathway between the low- and high-pressure systems, as shown in the weather chart on 19 August. These results indicated that strong northerly winds produced by the arrangement with the high-pressure system on the west side and the low-pressure system on the east side were a driving force for the rapid southward transport of the low-CO_2 to Minamitorishima. The same synoptic weather pattern over the northern part of the western North Pacific was found in all of the other ELC events for the transport pathway in the N sector. This weather pattern appears several times a month in summer, although it was more frequent in August than July.

[32] In the case of the transport pathway from the W sector, Figures 7c and 7d show the weather charts at 0000 UTC on 3 and 7 July 2002 before the ELC event observed on 10 July at Minamitorishima. The trajectory for this event indicates that the air masses over northern China moved slowly eastward across Japan to the Pacific and were then suddenly transported southward to Minamitorishima. The weather chart on 3 July one week before the event revealed that the eastward transport of continental air masses occurred north of a long Mei-yu front along about 35°N that was usually stationary from late June to early July over this region. However, the Mei-yu front in the weather chart on 7 July broke down at around 150°E, and the air masses suddenly moved toward the south through the rift of the front. The rapid southward transport was driven by strong northerly winds produced by the arrangement with the high-pressure system on the west side and the low-pressure system on the east side. This arrangement of pressure systems was similar to that in the case of the N sector, but the events in the W sector were relatively more frequent in July than those in the N sector because of the formation of a Mei-yu front.

[33] In the case of the transport pathway in the S sector, Figures 7e and 7f show the weather charts at 0000 UTC on 10 and 12 August 1999 before the ELC event observed on 17 August at Minamitorishima. The trajectory for this event indicated that an air parcel over the Philippine Islands rapidly moved northward and then turned to the east to proceed toward Minamitorishima. The weather chart on 10 August one week before the event revealed that the rapid northward movement of the air parcel was driven by strong southerly winds between the tropical depression over Japan and a high-pressure system over Minamitorishima. After the northward shift of the depression on 12 August, the air parcel moved eastward along the rim of the high-pressure system. This case suggested that the tropical depression played an important role in the northward transport of low-CO_2 influenced by the tropical region.

3.6. The 3-D Model Approaches

[34] In order to examine the spatial scale of the ELC events observed at Minamitorishima, the CO_2 distribution was simulated by a 3-D chemical transport model with biospheric fluxes. Figure 8 shows hourly CO_2 data at Minamitorishima from the model calculation in 2001 in comparison with the observed data. The two ELC events on 6 July and 23 August as well as the seasonal cycle were well reproduced in the model result. In particular, the magnitude and timing of the decreased CO_2 for the ELC events are quite similar between the model and the observation in 2001. The ELC events in 2002 are also captured accurately, indicating intrusions of low-CO_2 air masses largely influ-

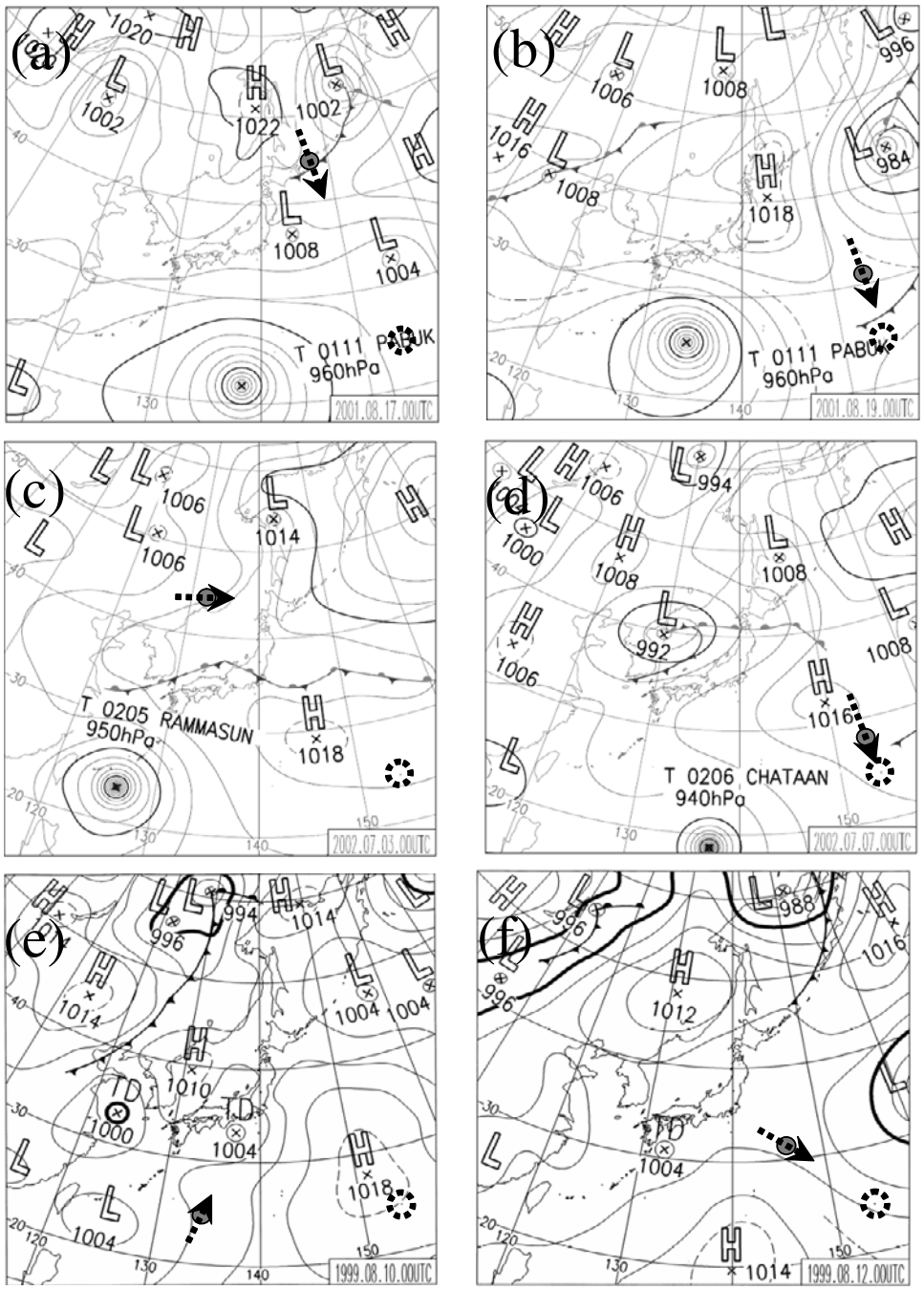

Figure 7. Surface weather charts before the ELC events observed at Minamitorishima on (a) 17 and (b) 19 August 2001 as trajectory type N, on (c) 3 and (d) 7 July 2002 as trajectory type W, and on (e) 10 and (f) 12 August 1999 as trajectory type S. The gray and dashed circles represent locations of air masses calculated by the backward trajectory analysis and Minamitorishima station, respectively. The weather charts were created by the Japan Meteorological Agency.

enced by biological uptake on land. When we used total CO_2 fluxes including anthropogenic emissions and ocean fluxes for the model calculation, the magnitude of ΔCO_2 minimum for the ELC events was reduced by 0.3 to 1.9 ppm that corresponded to 10 to 28% for the amplitudes of the decreased CO_2 peaks. It is strongly suggested that anthropogenic CO_2 emissions somewhat weaken biological uptake signal for the ELC events, although their anthropogenic influence may depend on the transport pathways over the continent.

[35] Figure 9 shows the global distributions of surface CO_2 for the ELC events produced by the model at 1200 UTC on 7 July 0600 UTC and 22 August 2001, respectively. It is clearly revealed that Minamitorishima during both ELC events was covered by a large stream with low CO_2 that extended southward from the high latitudes, but their low-CO_2 origins were different from

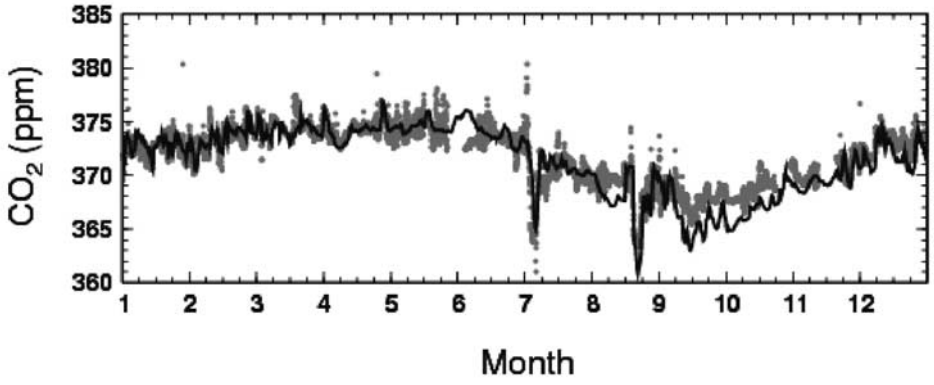

Figure 8. Comparison of hourly CO_2 data in 2001 between the observation (dots) and the 3-D model results (solid line).

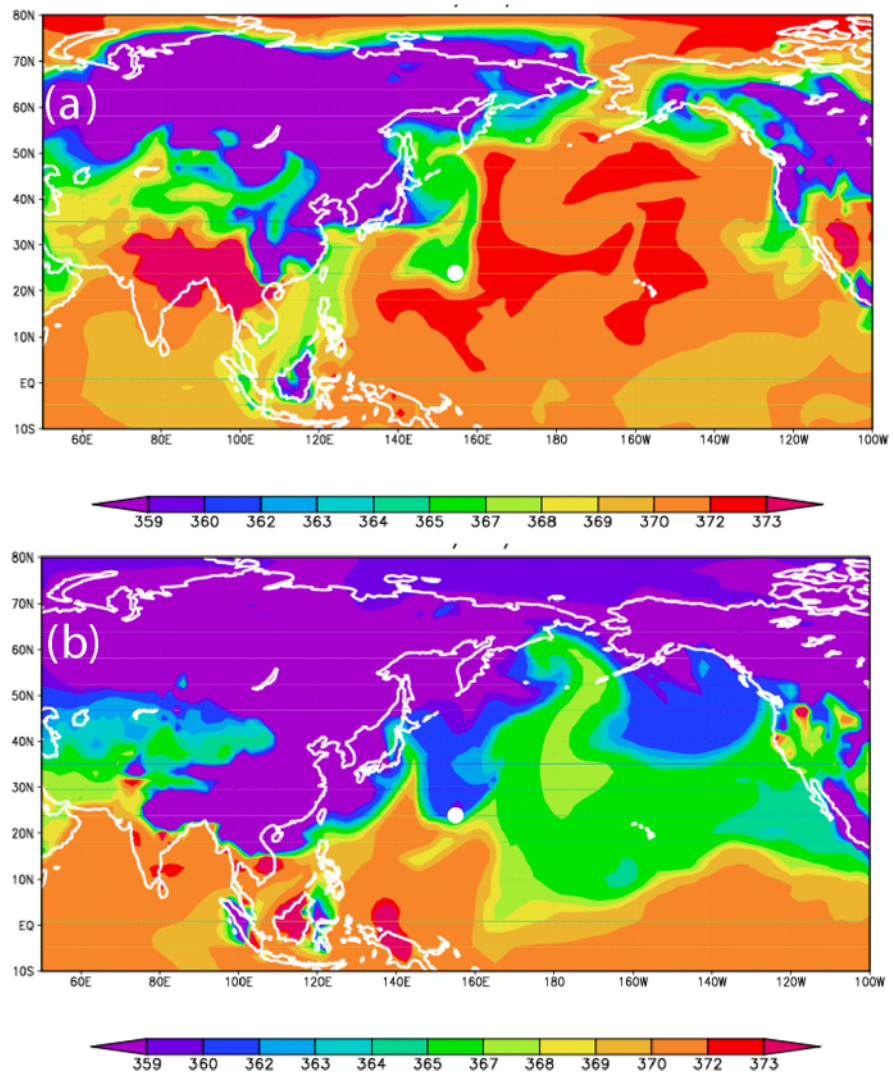

Figure 9. Spatial surface CO_2 distributions obtained by the 3-D model at (a) 0600 UTC on 7 July and (b) 1200 UTC 22 August 2001 when the low CO_2 events were observed. The white circle in each plot represents the location of Minamitorishima.

each other. In the case of the ELC event in July, the low CO_2 flowed out from the northern part of China to the western North Pacific and then turned south to proceed toward Minamitorishima. On the other hand, the ELC event in August showed that the low-CO_2 outflows from the strong CO_2 sinks in Siberia widely distributed over the western North Pacific and branched to the southward transport toward Minamitorishima.

[36] It was determined in both ELC events that the low-CO_2 stream around the Minamitorishima station spread out longitudinally between 140°E and 165°E (Figure 9). However, the low-CO_2 stream did not expand southward across the subtropical region around 20°N. In this western North Pacific, the Intertropical Convergence Zone (ITCZ) shifts northward to about 20°N during the summer season, as reported by the climatology of the highly reflective cloud data set [*Waliser and Gautier*, 1993]. The outgoing longwave radiation (OLR) data during the both ELC events in 2001 provided by the NOAA/OAR/ESRL (http://www.cdc.noaa.gov/) showed that high cloud belt indicative of the ITCZ was located in the subtropics between 20°N and 10°N over the western North Pacific. It appears that the ITCZ around the subtropics blocked further southward transport of the low CO_2 through the surface air and was then conveyed upward into the middle and upper troposphere.

4. Conclusions

[37] In this study, the long-term observational record of atmospheric CO_2 at Minamitorishima in the western North Pacific was analyzed to focus on the origin and transport mechanism of extremely low CO_2 (ELC) events. When the ELC events were extracted using a criterion of more than 3.1 ppm below the seasonal cycle, 40 events were found for the 11 year period from 1994 to 2004. Most ELC events occurred in summer between July and September, although the number of the events varied from year to year. Using 10-day backward trajectory analyses, air masses for ELC events were classified into 5 transport pathways of the N, W, S, E, and C sectors. In addition, the air mass origins for the 5 trajectory categories were consistent with the variations of CO, CH_4, and O_3 observed simultaneously at Minamitorishima.

[38] The trajectory and chemical analyses indicate that the low-CO_2 air masses were formed by the active uptake of CO_2 by the land biosphere over several different sink regions, such as Siberia, northern China, and Southeast Asia. The long-range transport from these continental sink regions to Minamitorishima was driven by rapid north-to-south or south-to-north movement of air masses. Such transport occasionally occurred in summer because of the arrangement of the low- and high-pressure systems over the western North Pacific. This transport mechanism for the ELC event was apparently different from the frequent outflow of Asian pollution driven by the moving spring cold fronts [e.g., *Bey et al.*, 2001; *Liang et al.*, 2004]. The ELC events in 2001 and 2002 were accurately reproduced by the 3-D model calculation. This calculation clearly revealed that the widespread distribution of the low CO_2 was prevented by the ITCZ in the subtropics over the western North Pacific in summer.

[39] The results of the present study suggested that the ELC event is an important process for the vigorous mixing of CO_2 in the interior of the Northern Hemisphere in the summer. In particular, the western North Pacific played an important role in the rapid exchange of CO_2 between the high latitudes and subtropical regions because of synoptic-scale weather changes. Thus, to learn more about global CO_2 circulation, it will be necessary to focus on short-term variations on the basis of continuous observations.

[40] **Acknowledgments.** We would like to acknowledge all members of the Japan Meteorological Agency for operating the trace gas measuring systems at Minamitorishima station. We also thank the anonymous reviewers for their valuable comments on this manuscript.

References

Andres, R. J., G. Marland, I. Fung, and E. Matthews (1996), A 1° × 1° distribution of carbon dioxide emissions from fossil fuel consumption and cement manufacture, 1950–1990, *Global Biogeochem. Cycles*, *10*(3), 419–429.

Bey, I., D. J. Jacob, J. A. Logan, and R. M. Yantosca (2001), Asian chemical outflow to the Pacific in spring: Origins, pathways, and budgets, *J. Geophys. Res.*, *106*(D19), 23,097–23,113.

Bousquet, P., P. Peylin, P. Ciais, C. Le Quéré, P. Friedlingstein, and P. P. Tans (2000), Regional changes in carbon dioxide fluxes of land and oceans since 1980, *Science*, *290*, 1342–1346.

Conway, T. J., P. P. Tans, L. S. Waterman, K. W. Thoning, D. R. Kitzis, K. A. Masarie, and N. Zhang (1994), Evidence for interannual variability of the carbon cycle from the National Oceanic and Atmospheric Administration/Climate Monitoring and Diagnostics Laboratory Global Air Sampling Network, *J. Geophys. Res.*, *99*(D11), 22,831–22,855.

Dlugokencky, E., L. P. Steele, P. M. Lang, and K. A. Masarie (1994), The growth rate and distribution of atmospheric methane, *J. Geophys. Res.*, *99*(D8), 17,021–17,043.

Dlugokencky, E. J., R. C. Myers, P. M. Lang, K. A. Masarie, A. M. Crotwell, K. W. Thoning, B. D. Hall, J. W. Elkins, and L. P. Steele (2005), Conversion of NOAA atmospheric dry air CH_4 mole fractions to a gravimetrically prepared standard scale, *J. Geophys. Res.*, *110*, D18306, doi:10.1029/2005JD006035.

Fung, I. Y., J. John, J. Lerner, E. Matthews, M. Prather, L. P. Steele, and P. J. Fraser (1991), Three-dimensional model synthesis of the global methane cycle, *J. Geophys. Res.*, *96*(D7), 13,033–13,065.

Gurney, K. R., et al. (2002), Towards robust regional estimates of CO_2 sources and sinks using atmospheric transport models, *Nature*, *415*, 626–630.

Gurney, K. R., et al. (2004), Transcom 3 inversion intercomparison: Model mean results for the estimation of seasonal carbon sources and sinks, *Global Biogeochem. Cycles*, *18*, GB1010, doi:10.1029/2003GB002111.

Harris, J. M., and J. D. Kahl (1990), A descriptive atmospheric transport climatology for the Mauna Loa observatory, using clustered trajectories, *J. Geophys. Res.*, *95*(D9), 13,651–13,667.

Harris, J. M., P. P. Tans, E. J. Dlugokencky, K. A. Masarie, P. M. Lang, S. Whittlestone, and L. P. Steele (1992), Variations in atmospheric methane at Mauna Loa observatory related to long-range transport, *J. Geophys. Res.*, *97*(D5), 6003–6010.

Higuchi, K., S. Murayama, and S. Taguchi (2002), Quasi-decadal variation of the atmospheric CO_2 seasonal cycle due to atmospheric circulation changes: 1979–1998, *Geophys. Res. Lett.*, *29*(8), 1173, doi:10.1029/2001GL013751.

Intergovernmental Panel on Climate Change (2001), *Climate Change 2001: The Scientific Basis: Contribution of Working Group I to the Third Assessment Report of the Intergovernmental Panel on Climate Change*, edited by J. T. Houghton et al., 881 pp., Cambridge Univ. Press, New York.

Jaffe, D., A. Mahura, J. Kelley, and J. Atkins (1997), Impact of Asian emissions on the remote North Pacific atmosphere: Interpretation of CO data from Shemya, Guam, Midway and Mauna Loa, *J. Geophys. Res.*, *102*(D23), 28,627–28,635.

Japan Meteorological Agency (1994), Summary report on the background air pollution monitoring by the Japan Meteorological Agency (in Japanese), *Sokkou Jiho*, *61*(4), 145–179.

Law, R. M., P. J. Rayner, P. L. Steele, and I. G. Enting (2002), Using high temporal frequency data for CO_2 inversions, *Global Biogeochem. Cycles*, *16*(4), 1053, doi:10.1029/2001GB001593.

Liang, Q., L. Laeglé, D. A. Jaffe, P. Weiss-Penzias, and A. Heckman (2004), Long-range transport of Asian pollution to the northeast Pacific:

Seasonal variations and transport pathways of carbon monoxide, *J. Geophys. Res.*, *109*, D23S07, doi:10.1029/2003JD004402.

Liu, H., D. J. Jacob, I. Bey, R. Yantosca, B. N. Duncan, and G. W. Sachse (2003), Transport pathways for Asian pollution outflow over the Pacific: Interannual and seasonal variations, *J. Geophys. Res.*, *108*(D20), 8786, doi:10.1029/2002JD003102.

Matsueda, H., H. Y. Inoue, and M. Ishii (2002), Aircraft observation of carbon dioxide at 8–13 km altitude over the western Pacific from 1993 to 1999, *Tellus, Ser. B*, *54*, 1–21.

Matsueda, H., et al. (2004a), Re-evaluation for scale and stability of CO_2 standard gases used as long-term observations at the Japan Meteorological Agency and the Meteorological Research Institute (in Japanese), *Tech. Rep. Meteorol. Res. Inst.*, *45*, 1–64.

Matsueda, H., Y. Sawa, A. Wada, H. Y. Inoue, K. Suda, Y. Hirano, K. Tsuboi, and S. Nishioka (2004b), Methane standard gases for atmospheric measurements at the MRI and JMA and intercomparison experiments, *Pap. Meteorol. Geophys.*, *54*, 91–109.

Murayama, S., K. Harada, K. Gotoh, T. Kitao, T. Watai, and S. Yamamoto (2003), On large variations in atmospheric CO_2 concentration observed over the central and western Pacific Ocean, *J. Geophys. Res.*, *108*(D8), 4243, doi:10.1029/2002JD002729.

Murayama, S., S. Taguchi, and K. Higuchi (2004), Interannual variation in the atmospheric CO_2 growth rate: Role of atmospheric transport in the Northern Hemisphere, *J. Geophys. Res.*, *109*, D02305, doi:10.1029/2003JD003729.

Nakazawa, T., S. Aoki, S. Murayama, M. Fukabori, T. Yamanouchi, H. Murayama, M. Shiobara, G. Hashida, S. Kawaguchi, and M. Tanaka (1991a), The concentration of atmospheric carbon dioxide at the Japanese Antarctic Station, Syowa, *Tellus, Ser. B*, *43*, 126–135.

Nakazawa, T., K. Miyashita, S. Aoki, and M. Tanaka (1991b), Temporal and spatial variations of upper tropospheric and lower stratospheric carbon dioxide, *Tellus, Ser. B*, *43*, 106–117.

Novelli, P. C., K. A. Masarie, P. M. Lang, B. D. Hall, R. C. Myers, and J. W. Elkins (2003), Reanalysis of tropospheric CO trends: Effects of the 1997–1998 wildfires, *J. Geophys. Res.*, *108*(D15), 4464, doi:10.1029/2002JD003031.

Pochanart, P., J. Hirokawa, Y. Kajii, and H. Akimoto (1999), Influence of regional-scale anthropogenic activity in northeast Asia on seasonal variations of surface ozone and carbon monoxide observed at Oki, Japan, *J. Geophys. Res.*, *104*(D3), 3621–3631.

Randerson, J. T., M. V. Thompson, T. J. Conway, I. Y. Fung, and C. B. Field (1997), The contribution of terrestrial sources and sinks to trends in the seasonal cycle of atmospheric carbon dioxide, *Global Biogeochem. Cycles*, *11*, 535–560.

Sawa, Y. (2005), A study of variations and transport of carbon monoxide in the free troposphere over the western Pacific, D.Sc. thesis, Fac. Sci., Tohoku Univ., Sendai, Japan.

Sawa, Y., H. Matsueda, Y. Makino, H. Y. Inoue, S. Murayama, M. Hirota, Y. Tsutsumi, Y. Zaizen, M. Ikegami, and K. Okada (2004), Aircraft observation of CO_2, CO, O_3 and H_2 over the North Pacific during the PACE-7 campaign, *Tellus, Ser. B*, *56*, 2–20.

Taguchi, S. (1996), A three-dimensional model of atmospheric CO_2 transport based on analyzed winds: Model description and simulation results for TRANSCOM, *J. Geophys. Res.*, *101*(D10), 15,099–15,110.

Taguchi, S., H. Matsueda, H. Y. Inoue, and Y. Sawa (2002a), Long-range transport of CO from tropical ground to upper troposphere: A case study for Southeast Asia in October 1997, *Tellus, Ser. B*, *54*, 22–40.

Taguchi, S., T. Iida, and J. Moriizumi (2002b), Evaluation of the atmospheric transport model NIRE-CTM-96 by using measured radon-222 concentrations, *Tellus, Ser. B*, *54*, 250–268.

Taguchi, S., S. Murayama, and K. Higuchi (2003), Sensitivity of interannual variation of CO_2 seasonal cycle at Mauna Loa to atmospheric transport, *Tellus, Ser. B*, *55*, 547–554.

Takahashi, T., et al. (2002), Global sea-air CO_2 flux based on climatological surface ocean pCO_2, and seasonal biological and temperature effects, *Deep Sea Res. II*, *49*(9–10), 1601–1622.

Tanaka, M., T. Nakazawa, M. Shiobara, H. Ohshima, S. Aoki, S. Kawaguchi, T. Yamanouchi, Y. Makino, and H. Murayama (1987a), Variations of atmospheric carbon dioxide concentration at Showa Station (69°00′S, 39°35′E), Antarctica, *Tellus, Ser. B*, *39*, 72–79.

Tanaka, M., T. Nakazawa, and S. Aoki (1987b), Seasonal and meridional variations of atmospheric carbon dioxide in the lower troposphere of the northern and southern hemispheres, *Tellus, Ser. B*, *39*, 29–41.

Tanaka, M., T. Nakazawa, and S. Aoki (1989), Time and space variations of tropospheric carbon dioxide over Japan, *Tellus, Ser. B*, *39*, 3–12.

Tanimoto, H., Y. Sawa, H. Matsueda, I. Uno, T. Ohara, K. Yamaji, J. Kurokawa, and S. Yonemura (2005), Significant latitudinal gradient in the surface ozone spring maximum over East Asia, *Geophys. Res. Lett.*, *32*, L21805, doi:10.1029/2005GL023514.

Waliser, D. E., and C. Gautier (1993), A satellite-derived climatology of the ITCZ, *J. Clim.*, *6*, 2162–2174.

Watanabe, F., O. Uchino, Y. Joo, M. Aono, K. Higashijima, Y. Hirano, K. Tsuboi, and K. Suda (2000), Interannual variation of growth rate of atmospheric carbon dioxide concentration observed at the JMA's three monitoring stations: Large increase in concentration of atmospheric carbon dioxide in 1998, *J. Meteorol. Soc. Jpn.*, *78*, 673–682.

H. Matsueda and Y. Sawa, Geochemical Research Department, Meteorological Research Institute, 1-1 Nagamine, Tsukuba-shi, Ibaraki-ken 305, Japan.

S. Murayama and S. Taguchi, National Institute of Advanced Industrial Science and Technology, 16-3 Onogawa, Tsukuba 305-8569, Japan.

S. Okubo, Nagano Local Meteorological Observatory, Japan Meteorological Agency, 1-8-18 Hakosimizu, Nagano, Japan.

Y. Tsutsumi, Global Environment and Marine Department, Japan Meteorological Agency, 1-3-4 Otemachi, Chiyoda-ku, Tokyo 100-8122, Japan.

A. Wada, Meteorological College, 7-4-81 Asahi-cho, Kashiwa, Chiba 277-0852, Japan. (awada@mc-jma.go.jp)